Ocean and atmosphere influence on the 2015 European heatwave

Environmental Research Letters

LETTER

Ocean and atmosphere influence on the 2015 European heatwave

J V Mecking[1,2], S S Drijfhout[1,3,4], J J-M Hirschi[2] and A T Blaker[2]

[1] Ocean and Earth Science, National Oceanography Centre Southampton, University of Southampton, Southampton, United Kingdom
[2] National Oceanography Centre, Southampton, United Kingdom
[3] Royal Netherlands Meteorological Institute, The Netherlands
[4] University of Utrecht, The Netherlands

E-mail: jennifer.mecking@noc.ac.uk

Keywords: seasonal predictions, European summer, 2015 heatwave, 2015 cold blob, North Atlantic SST

Supplementary material for this article is available online

OPEN ACCESS

RECEIVED
9 May 2019

REVISED
10 October 2019

ACCEPTED FOR PUBLICATION
11 October 2019

PUBLISHED
14 November 2019

Abstract

During the summer of 2015, central Europe experienced a major heatwave that was preceded by anomalously cold sea surface temperatures (SSTs) in the northern North Atlantic. Recent observation-based studies found a correlation between North Atlantic SST in spring and European summer temperatures, suggesting potential for predictability. Here we show, by using a high-resolution climate model, that ocean temperature anomalies, in combination with matching atmospheric and sea-ice initial conditions were key to the development of the 2015 European heatwave. In a series of 30-member ensemble simulations we test different combinations of ocean temperature and salinity initial states versus non-initialised climatology, mediated in both ensembles by different atmospheric/sea-ice initial conditions, using a non-standard initialisation method without data-assimilation. With the best combination of the initial ocean, and matching atmosphere/sea-ice initial conditions, the ensemble mean temperature response over central Europe in this set-up equals 60% of the observed anomaly, with 6 out of 30 ensemble-members showing similar, or even larger surface air temperature anomalies than observed.

1. Introduction

The importance of skilful seasonal forecasts is highlighted by the devastating socio-economic impacts of extreme summer conditions over Europe (Ciais *et al* 2005, Zampieri *et al* 2017). The heatwave of 2003 resulted in more than 70 000 deaths (Robine *et al* 2008) and similar numbers apply to the Russian heatwave of 2010 (Grumm 2011). In the summer of 2015, Europe experienced a heatwave ranking third warmest on record, surpassed only by the summers of 2003 and 2010 (Russo *et al* 2015). The heatwave began in late June in Western Europe and then spread towards Southern and Eastern Central Europe, with several cities reporting record high temperatures (Sippel *et al* 2016). The exceptionally warm conditions led to extreme drought over most of central Europe (Orth *et al* 2016) with several heat-related deaths (Muthers *et al* 2017, Urban *et al* 2017, Výberči *et al* 2018). With future climate projections estimating mean summer temperatures over Europe to increase by 0.6°–1.5 °C in 2016–2035 (Kirtman *et al* 2013), heatwaves will become more common (Meehl and Tebaldi 2004, Schär *et al* 2004, Ballester *et al* 2010, Lhotka *et al* 2018).

To date winter forecasts yield greater seasonal prediction skill than summer forecasts (Scaife *et al* 2014, Stockdale *et al* 2015, O'Reilly *et al* 2017). However, several recent studies have noted a connection between the winter/spring sea surface temperatures (SSTs) in the Atlantic Ocean and conditions over Europe (Feudale and Shukla 2011, Gastineau and Frankignoul 2015, Ossó *et al* 2018). In the months leading up to the exceptionally warm summer of 2015 an anomalous 'cold blob' was present in the northern part of the North Atlantic (Josey *et al* 2018). It was argued that the resulting anomalous gradient in SST phase-locked a meander in the jet stream, leading to the warmer temperatures over Europe (Buchan *et al* 2014, Duchez *et al* 2016).

Here, we investigate whether the 2015 European heatwave can be re-forecasted using an alternative

initialisation method that does not make use of data-assimilation. The rationale behind this choice is that the ocean is an almost purely adiabatic system below the surface mixed-layer. As a consequence, the slowly varying ocean circulation contains both surface and subsurface temperature and salinity anomalies, with the potential for subsurface anomalies to be mixed up to the surface where they interact with the atmosphere and may contribute to skilful predictions (e.g. Grist *et al* 2019). Hence our choice to test a gentler initialisation method where neither ocean nor atmospheric initial conditions are nudged towards observations by artificial sources and sinks. In this study we focus on the link between ocean and atmosphere initial conditions and how it may affect the summer re-forecast. A set of ensemble experiments using the coupled climate model HadGEM3-GC2 (Williams *et al* 2015) are performed using various ocean and atmosphere initial conditions. In contrast to previous studies the ocean is initialised using an anomaly initialisation technique whereby anomalies from a forced ocean-only simulation are introduced to the coupled model restart. In addition, this initialisation method allows for separating the influence of ocean, sea-ice, land-surface (soil moisture) and atmosphere initialisation. Studies have shown that land surface properties such as soil moisture also influence heatwaves (e.g. Quesada *et al* 2012, Ardilouze *et al* 2017), and may therefore provide an important source of predictability for heatwaves. However, since our experiments require a coupled high-resolution prediction model, we decided to focus all our available computational resources on ocean, sea-ice and atmosphere initialisation only.

2. Methods and data

2.1. Model setup

To investigate the potential link between patterns of anomalous North Atlantic SST and European summer heatwaves we conduct a set of experiments using the coupled climate model HadGEM3-GC2 (Williams *et al* 2015), consisting of atmosphere, ocean, sea-ice and land-surface models. The ocean configuration is Global Ocean 5.0 (Megann *et al* 2014), which is based on NEMO v3.4 (Madec 2015) and uses the ORCA025 (nominally ¼°) tripolar grid configuration. The atmosphere model is the Met Office unified model with the Global Atmosphere v6.0 (Walters *et al* 2017) that has a horizontal resolution of N216 (approximately 60 km) and 85 vertical levels. This model setup is used in the seasonal forecasting system, DEPRESYS at the Met Office but with the addition of data assimilation (Dunstone *et al* 2016).

2.2. Initialisation approach

We use a new method to initialise our experiments, taking anomaly fields from a forced ocean-only simulation (Garry *et al* 2019) with the same ocean model as used in the coupled model. Thereafter, these anomalies are added to the climatological mean of the ocean in the coupled model to generate an initial state. By introducing the anomalies in this way, we minimise initial shocks and model drift and we avoid the need for drift correction, data assimilation or nudging towards a particular field. This approach is in contrast to previous studies where the ocean is either initialised using the full fields from a forced ocean-only experiment (Matei *et al* 2012) or anomalies based on observations (Magnusson *et al* 2013, Smith *et al* 2013).

We generate 5 different ocean initial conditions: a control ocean initial condition where climatological three-dimensional (3D) ocean temperature and salinity averaged over April/May from 1981 to 2010 are taken from a historical + RCP4.5 simulation of the coupled model (CLIM) and four experiments where 3D temperature and salinity anomalies on 1st May from a forced ocean-only simulation (driven by an atmospheric reanalysis product; Garry *et al* 2019) are added to the CLIM ocean initial condition. The temperature anomalies from the ocean initial conditions are computed as the difference between the forced ocean-only simulation restart file and April/May means averaged from 1981 to 2010. The ocean anomaly fields are taken from four years: 2015, 2014, 1993 and 1984, (figures 1(b) and 2). For each of these initial states we run a 30-member initial condition perturbation ensemble, adding spatially varying white noise. The amplitude of the white noise was chosen to be equal to the standard deviation of differences in SST in consecutive 5 days means from the NEMO hindcast, which is a typical timescale of mesoscale variability in the ocean. The noise was linearly tapered to zero over the upper 50 m of the ocean and then added to the ocean initial state, to prevent the anomalies from disappearing quickly. The perturbed SSTs immediately transfer the noise to the atmosphere leading to sufficient spread in the ensemble. Focusing on the ocean initial state we decided it was more appropriate to add a realistic noise pattern to the ocean initial fields. Any convective instabilities arising from the initialisation were removed from the 3D temperature and salinity initial condition fields using the same method as in the NEMO ocean model code. Each ensemble member was then computed for 5 months, starting from 1st May.

The atmospheric initial conditions (which in our setup include the states of atmosphere, sea ice and land) are taken on 1st May in the years of 2015, 1992 and 1986 in the coupled HadGEM3 historical + RCP4.5 simulation. Note that, apart from the external forcing, atmospheric states for each year in HadGEM3 bear no resemblance to the climate of the real world in the corresponding year. Similarly, the ocean states in these HadGEM3 runs are unrelated to the ocean state in the ocean-only forced run of that same year. Therefore, in the remainder of this paper we will refer to the three

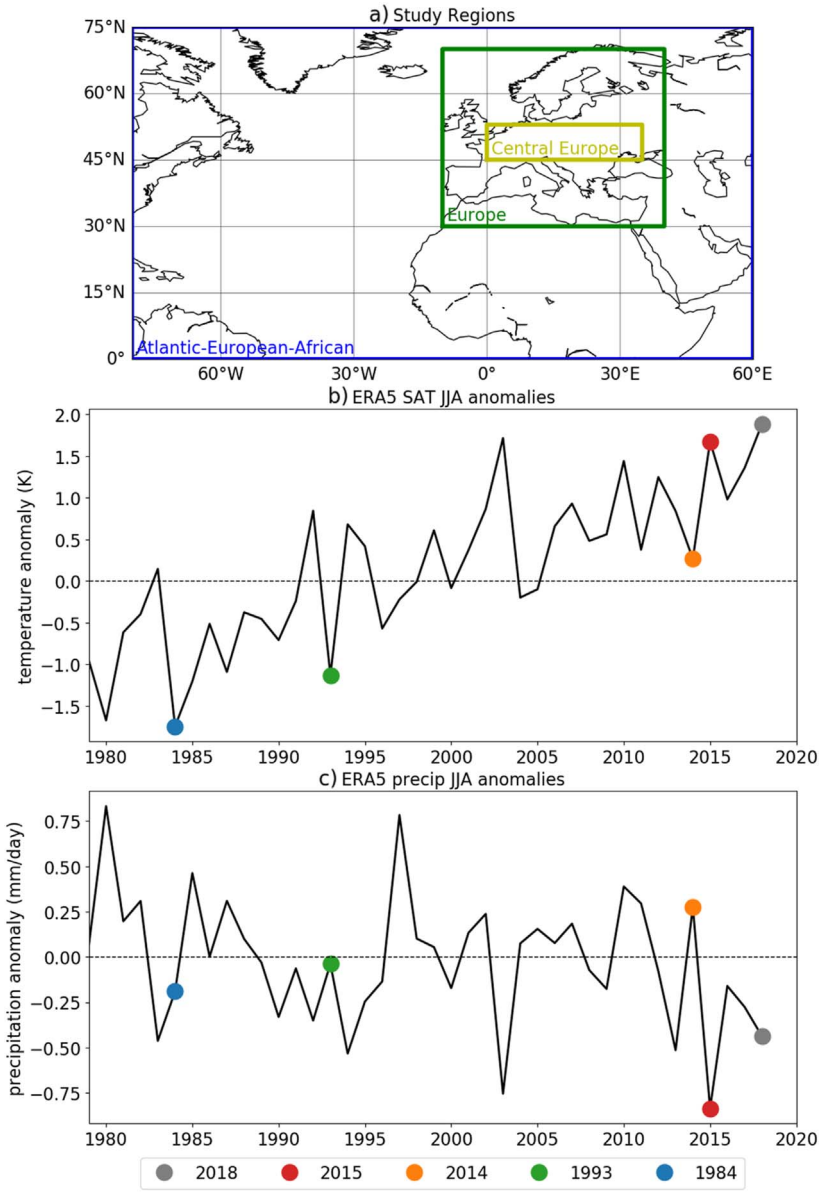

Figure 1. (a) Regions used for calculations in this study, central European box (0°−35 °E, 45°−53 °N, yellow), European region (10 °W–40°E, 30°–70 °N, green) and Atlantic-European-African (A-E-A, 80 °W–60°E, 0°−75 °N, blue). Time series of the mean June, July and August (JJA) (b) surface air temperature (SAT) from ERA5 and (c) precipitation from ERA5 averaged over central Europe (see panel (a)). The data are presented as an anomaly with respect to the 1981–2010 mean. The coloured dots indicate the years used in this study from which the ocean was initialised and the grey dot for 2018.

atmospheric initial conditions as A (2015), B (1992) and C (1986).

We only vary the atmospheric and sea ice states in the initial conditions A, B, and C. Soil moisture also has an influence on heatwaves (Quesada *et al* 2012, Ardilouze *et al* 2017). However, here we initialise soil moisture from its climatological mean (1981–2010) in all experiments as this facilitates isolating the effect of ocean and atmosphere/sea-ice on the re-forecasts. This also allows us to keep computational cost within the limits of available HPC resources. Even without varying the initial state for soil moisture exploring the impact different combinations ocean and atmosphere initial conditions described above we have generated a total of 450 ensemble members across 15 different experiments.

To analyse the influence of the ocean anomalies on simulated temperatures over Europe, the ensemble-mean atmospheric response in the CLIM experiment is subtracted from the ensemble-mean atmospheric response of the anomalously initialised runs for each ocean initial state and for each atmospheric initial condition separately, showing data averaged over JJA. We emphasise that in each case, the same atmospheric initial condition is used in both the initialised ensemble and the CLIM ensemble and that only the ocean state differs between the two ensembles. It is also important to note that the external forcing used in

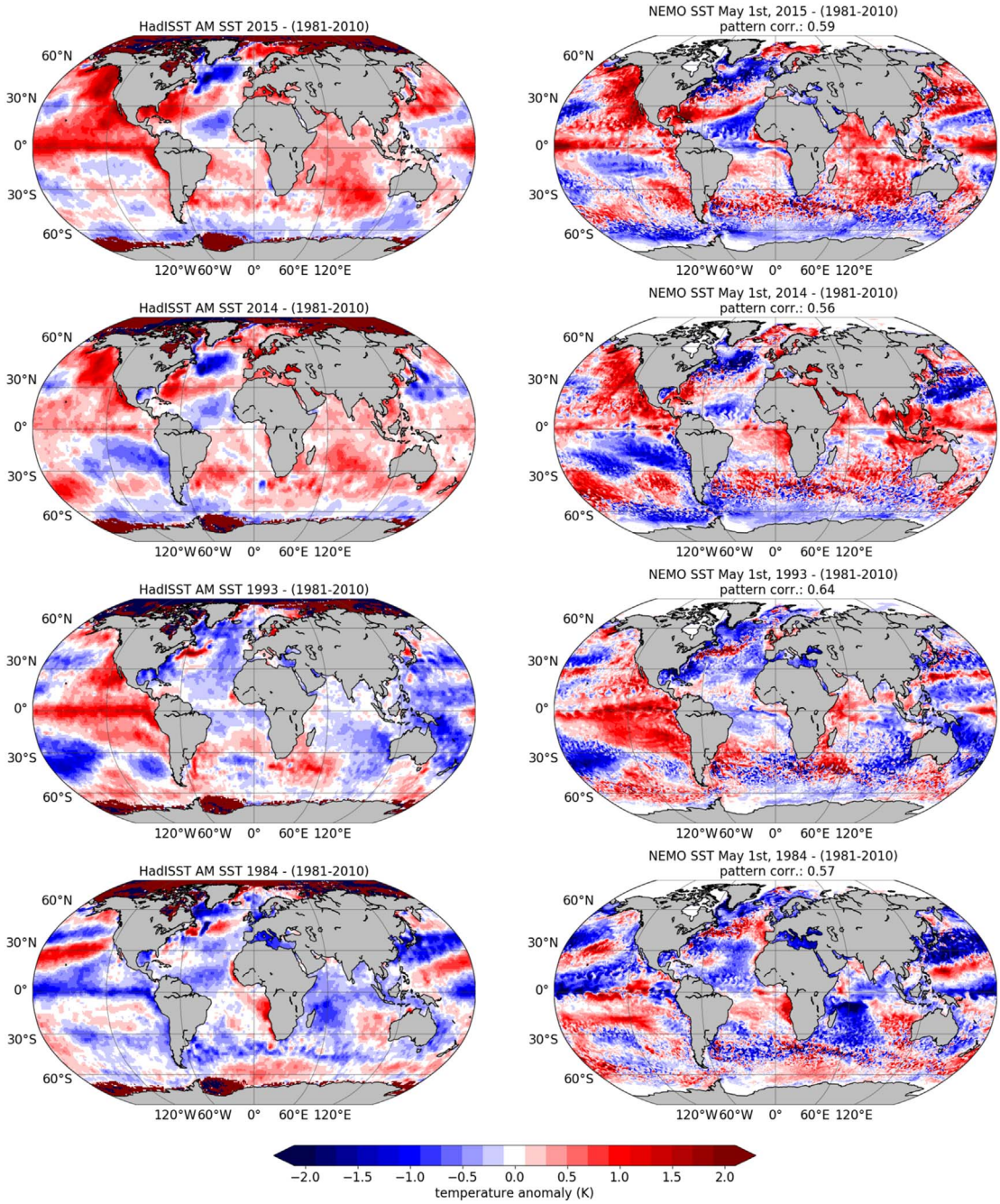

Figure 2. Left column April–May mean SST from HadISST data and right column shows 1st May ocean initial condition anomaly for the years 2015, 2014, 1993 and 1984 ordered from top to bottom. The pattern correlation between the HadISST data and 1st May ocean restart is shown in the title in the right column.

these experiments is based on 1978 for all ensemble members, therefore the only impact seen from external forcing is the fingerprint they have left on the ocean initial conditions. The main focus is on the impact of ocean initial conditions, mediated by a small set of different atmosphere and sea-ice states, on the exceptionally warm summer of 2015.

2.3. Observation-based data

For comparisons with observations, daily surface air temperature (SAT), precipitation and SST data from ERA5 (Copernicus Climate Change Service C3S 2017), SST from HadISST (Rayner *et al* 2003) and Arctic sea ice depth reanalysis dataset PIOMAS (Schweiger *et al* 2011) were used. All observation-based anomalies are referenced to the time period 1981–2010.

2.4. Significance tests

The Kolmogorov–Smirnov test is used throughout the manuscript when testing the difference between two means. A significance level of 5% was used throughout this study. To test whether a correlation value is significant a Student's t-test is applied.

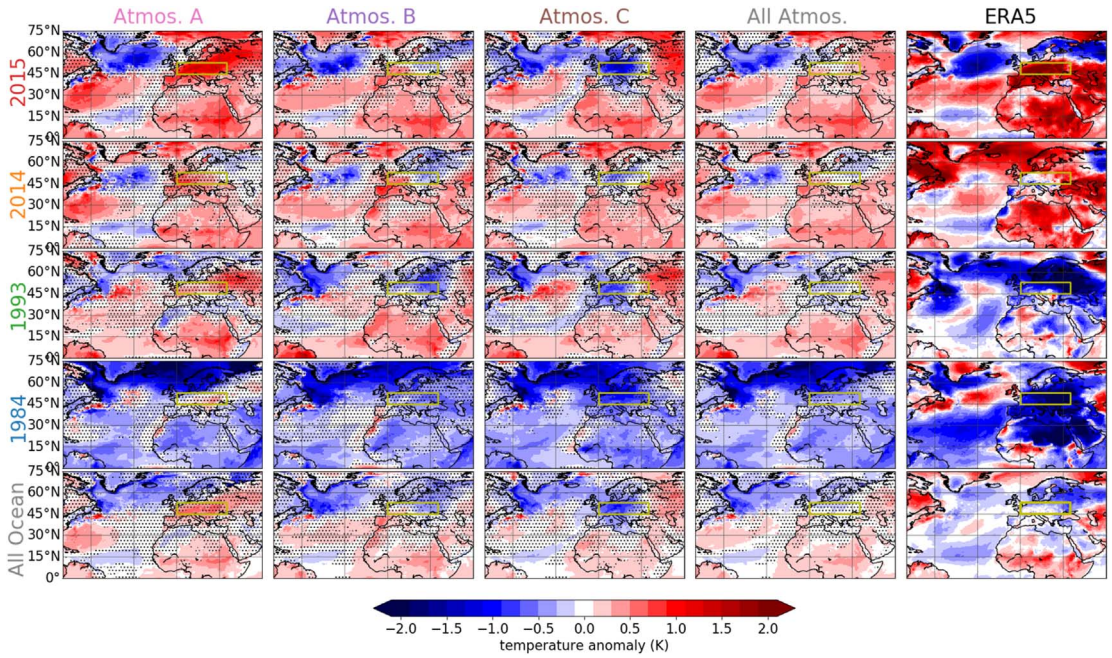

Figure 3. JJA SAT anomalies for all ocean (top 4 rows), the mean access all ocean initial conditions (bottom row), all atmosphere initial conditions (first 3 columns), the mean across all atmosphere initial conditions (fourth column) and in ERA5 computed with respect to the 1981–2010 mean. Regions where the difference is not significant at the 5% level are stippled in the first 4 columns. The yellow box indicates the region described as the Central European box.

3. Ocean state and the 2015 heatwave

To assess the impact of ocean initial conditions on the June, July and August (JJA) temperature anomalies over Europe we run seasonal re-forecasts for JJA, starting from four different ocean initial conditions (2015, 2014, 1993, 1984; see Methods). These ocean initial states preceded the second warmest summer since 1980 (2015), an average year (2014), and two colder than average years (1984 and 1993), with 1984 being the coldest since 1980. (figure 1(b)). The summer of 2015 also had the least precipitation since 1980; 2014 slightly wetter than average; 1984 slightly drier than average; and 1993 approximately average (figure 1(c)). Three of those 4 initial ocean states featured a warm eastern tropical Pacific with El Niño-like conditions (1993, 2014, 2015) and one initial state (1983) with La Nina-like conditions (figure 2). To assess how the atmospheric initial conditions affect the impact of ocean initialisation we use the three arbitrarily chosen atmospheric initial conditions from the model's historical + RCP4.5 simulation (A, B, C), which also include sea ice and climatological soil moisture values for land. The same atmospheric conditions are applied in both the experiment and the control ensemble, CLIM, so their effect is only indirect by the way they influence the evolution of the ocean anomalies and how these anomalies feed-back to the atmosphere.

Our series of re-forecast ensembles show that both the initial ocean and atmosphere conditions in May influence the JJA temperature anomalies (figure 3). When considering the entire Atlantic-European-African (A-E-A) domain (figure 1(a)) especially over the North Atlantic and Africa the JJA SAT anomaly patterns remain similar when atmospheric initial conditions are varied. Concentrating on the 2015 ocean conditions (figure 3, top row) the tripole pattern in the North Atlantic with warm anomalies between 15 °N and 45°N, flanked by cold anomalies to the north and south, is present for all atmospheric initial conditions. Similarly, the warm anomalies observed over much of Africa and the Middle-East are also simulated with all three atmospheres. This shows that in our experiments the ocean initial state in May imposes a strong constraint on the large-scale JJA SAT anomaly patterns, and on average this ocean state leads to pronounced JJA anomalies (figure 3, fourth column), which are significantly correlated with the JJA temperature anomaly patterns observed in the real world in 2015, 2014, 1993 and 1984 (figure 3, fifth column; figure 4(b)). It is also evident that there is a sensitivity to atmospheric conditions. Over the European region (defined in figure 1(a)) significant differences between the different ensembles arise. This is most evident in the ensemble using the 2015 ocean and atmospheric state C, where cold JJA SAT develop over much of Europe (figure 3, 3rd column, top), in contrast to the ensembles using atmospheres A and B. However, averaging over JJA anomalies obtained for the oceanic conditions 2015, 2014, 1993, and 1984 (figure 3, bottom row) gives rise to weaker mean anomalies than averaging over atmospheric initial conditions A, B, and C (figure 3, 4th column), over the larger A-E-A. This is

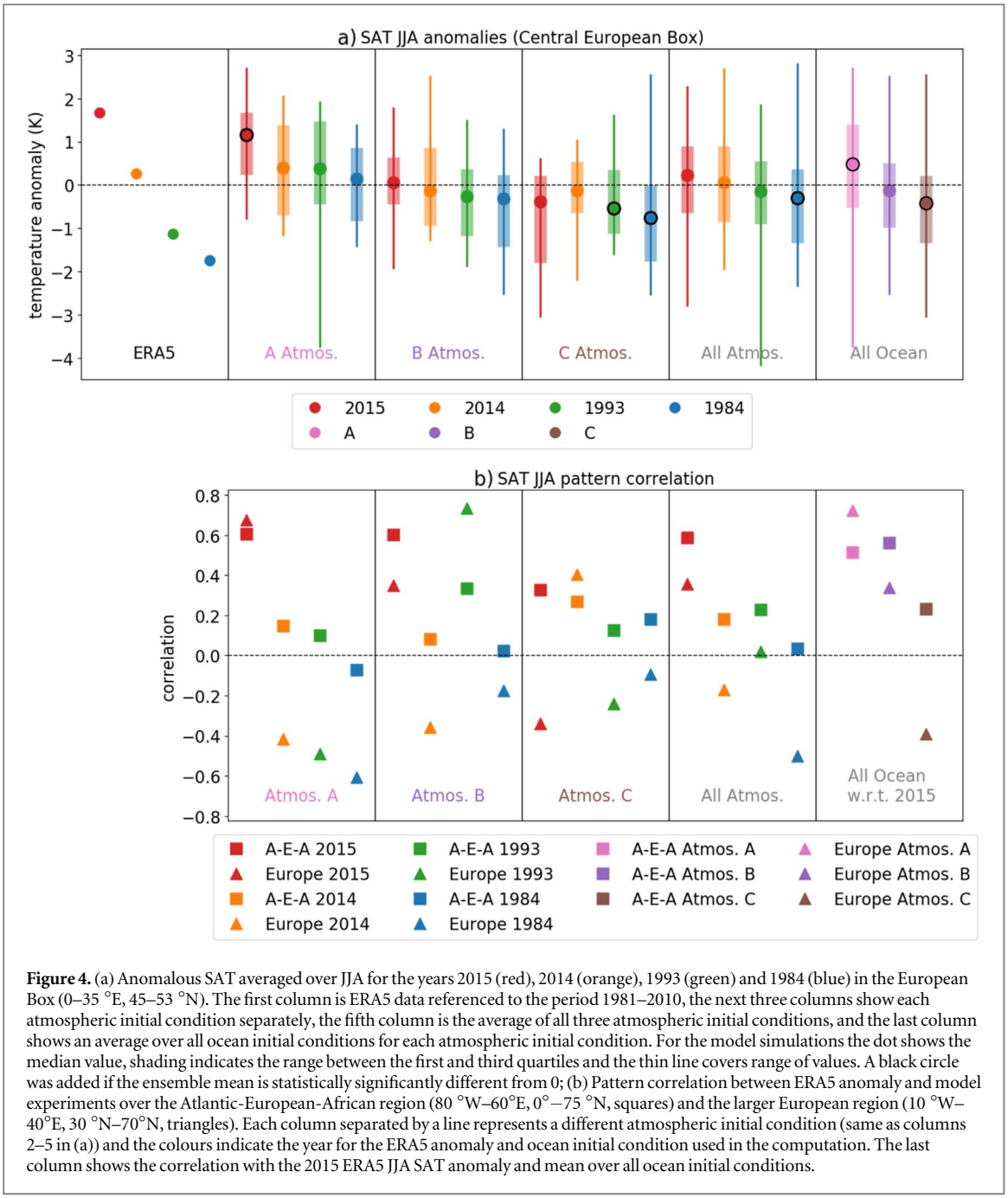

Figure 4. (a) Anomalous SAT averaged over JJA for the years 2015 (red), 2014 (orange), 1993 (green) and 1984 (blue) in the European Box (0–35 °E, 45–53 °N). The first column is ERA5 data referenced to the period 1981–2010, the next three columns show each atmospheric initial condition separately, the fifth column is the average of all three atmospheric initial conditions, and the last column shows an average over all ocean initial conditions for each atmospheric initial condition. For the model simulations the dot shows the median value, shading indicates the range between the first and third quartiles and the thin line covers range of values. A black circle was added if the ensemble mean is statistically significantly different from 0; (b) Pattern correlation between ERA5 anomaly and model experiments over the Atlantic-European-African region (80 °W–60°E, 0°–75 °N, squares) and the larger European region (10 °W–40°E, 30 °N–70°N, triangles). Each column separated by a line represents a different atmospheric initial condition (same as columns 2–5 in (a)) and the colours indicate the year for the ERA5 anomaly and ocean initial condition used in the computation. The last column shows the correlation with the 2015 ERA5 JJA SAT anomaly and mean over all ocean initial conditions.

not always the case over the central European box where the average over initial condition A gives a stronger JJA temperature signal than the average over the oceanic conditions 2015. This suggests that the atmospheric initial condition plays a role in obtaining the correct sign of the anomalies over central Europe. However, our results also show that to capture the magnitude of the heatwave getting the correct ocean initial conditions is essential (figures 3 and 4(a)). In general, it is difficult to see how the impact of atmospheric initial conditions could have a systematic effect on the re-forecasts, as the control ensemble always uses the same atmospheric initial states, unless the four ocean initial states have a signal in common. As can be seen in figure 2 and figure S1 (available online at stacks.iop.org/ERL/14/114035/mmedia) this common signal projects on an El Niño signal (see discussion).

Despite the sensitivity to atmospheric initial conditions, the JJA average SAT across all ensemble members and atmosphere initial conditions A and B shows that the predicted temperatures over Europe rank in the same order (2015, 2014, 1993, 1984) as the observations, although with a weaker amplitude, and differences between ocean initial conditions with the majority of the SAT anomalies are not statistically significantly different from 0 (figure 4(a)). Over the A-E-A region, the spatial patterns in re-forecasts and observations show several similarities (figure 4(b) squares), with all but one ensemble mean having a positive pattern correlation with the observations (figures 3 and 4(b)). When averaged over all ocean initial conditions,

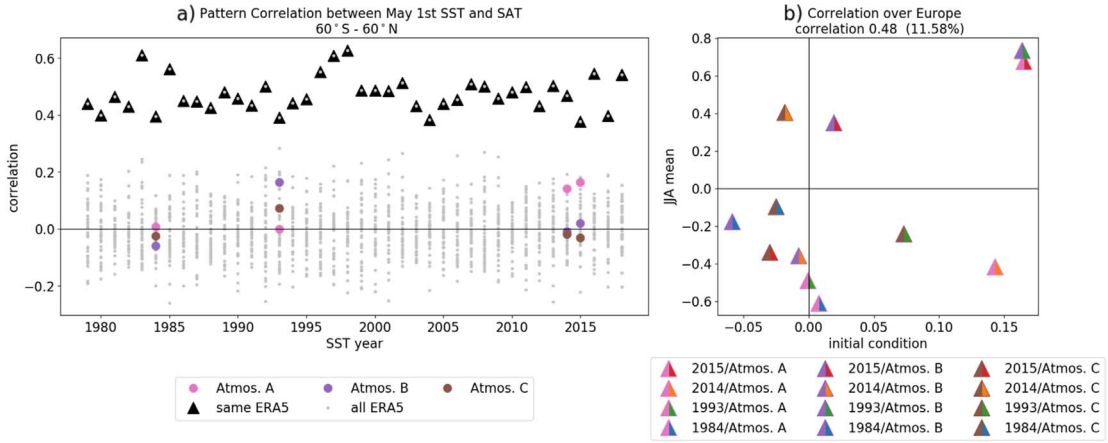

Figure 5. (a) Spatial pattern correlation between 1st May SAT and SST anomalies with respect to 1981–2010 mean computed globally between 60 °S and 60 °N. The grey dots show the pattern correlation for SAT for each year with the SST for the year specified on the *x*-axis and the black triangle is when the SST and SAT are taken from the same year using ERA5 data. The pink (Atmos. A), purple (Atmos. B) and brown (Atmos. C) dots show the pattern correlation between the SAT anomaly in the atmospheric initial condition and SST anomaly in the ocean initial condition used in the model simulations, with the *x*-axis specifying the year of the ocean initial condition. (b) The relationship between the 60 °S–60 °N pattern correlation of the initial conditions (*x*-axis) and the JJA mean SAT anomalies over the larger European Region (*y*-axis). The atmospheric initial conditions are indicated in pink, purple and brown on the left for Atmos. A, B and C and the ocean initial conditions are indicated in red, orange. green and blue on the right for 2015, 2014, 1993, and 1984, respectively.

predictions with atmospheric initial state A give anomalously warm temperatures over central Europe, but the amplitude is about half of what we find when atmospheric initial state A and ocean initial state for 2015 are used together (figure 3, 1st column top and bottom panel, figure 4(a)).

3.1. Successful re-forecast of summer 2015

For all atmospheric initial states our summer 2015 re-forecasts show anomaly patterns over the A-E-A region that are positively correlated with the observations (figures 3 and 4(b)), with ensemble mean pattern correlations between prediction and observation ranging from 0.32 to 0.61 (figure 4(b), squares). However, only the prediction using atmospheric initial state A was able to simulate the large spatial-scale warm anomaly over Europe (figure 3 top-left), with statistically significant warm JJA temperature anomalies over much of Europe. The ensemble-mean temperature anomaly in the central European box is 1.04 °C, which is more than half of what was observed (1.79 °C) and statistically significantly different from 0 (figure 4(a)), with 6 of the 30 ensemble members having temperature anomalies equal to or warmer than the observations. The ensemble-mean pattern of the 2015 summer temperature anomalies using atmosphere initial condition A closely matches the observed pattern of anomalous temperatures in JJA over the European region (pattern correlation of 0.68; figure 4(b), red triangle). Europe also experienced very dry conditions with record low precipitation falling over the central Europe box region in 2015 (figure 1(c)). The combination of the 2015 ocean initial condition and atmosphere initial condition A was also able to capture this exceptionally low precipitation over Europe with a statistically significant signal (figure S3).

The pattern correlations over the A-E-A region and the European region using the 2015 ocean initial condition and Atmospheric initial condition A (red square and triangle in the atmosphere initial condition A column in figure 4(b)) are similar to the pattern correlation computed from the average of all ocean initial conditions using atmosphere initial condition A and the 2015 ERA5 anomaly (pink square and triangle in the all ocean column in figure 4(b)). However, when considering pattern regressions instead we find that the amplitudes, and therefore regression values, are much weaker in the 'all ocean' column (figure S4). The consistent large-scale (A-E-A) temperature signal found when ocean conditions are kept the same whilst varying the atmospheric initial conditions suggest that ocean initial conditions are key to the successful seasonal re-forecast. At the same time our results also show that combining with the 'correct' atmospheric initial conditions matter. This implies that, when initialising a coupled seasonal forecasting system with ocean anomalies obtained from a forced ocean run, the anomalously warm SAT over central Europe in 2015 can be successfully modelled, but only when the 'correct' atmospheric initial state is used.

3.2. Matching ocean and atmospheric initial states

To investigate possible reasons why atmospheric initial condition A produced the best fit to the ocean initial condition of 1st May 2015, we calculated the pattern correlation between SAT and SST between 60 °S and 60 °N (avoiding regions covered by sea-ice) in the initial conditions. Using this metric three combinations stand out, 2015 ocean with atmosphere

A, 1993 ocean with atmosphere B and 2014 ocean with atmosphere A, (figure 5(a)). Two of the 3 atmosphere/ocean initial condition combinations with the highest pattern correlation also exhibit the highest pattern correlation between predicted JJA SAT anomalies and observed JJA SAT anomalies in the A-E-A region (figure 4(b), squares) and in the smaller European box (figures 4(b), 5(b) triangles); only the 2014 ocean with atmosphere A has a weak relationship to the observed JJA SAT anomalies (figure 4(b)). There is a correlation of 0.48, between the initial condition global pattern correlation (coloured dots from figure 5(a)) and the JJA ensemble mean pattern correlation with ERA5 in the European region (triangles in figure 4(b)) (figure 5(b)). This suggests that there is a relationship between the similarity of ocean and atmosphere initial conditions and the resulting SAT pattern (similar relationships are also seen with A-E-A region pattern correlation and regression (figure S5)). When performing the same computation with observation-based ERA5 data for 1st May and taking the SAT and SST anomalies from the same year the pattern correlation is always much higher (0.38–0.63) than correlating the SSTs of one year with the SAT patterns from another year (−0.26 to 0.28, figure 5(a)). This further motivates using the pattern correlation to determine the best atmosphere/ocean initial condition combination.

To increase confidence in this metric, we repeated the pattern correlation between all 1st May SAT snapshots (daily means) from the historial + RCP4.5 run with the SST in our 2015 ocean initial condition. Taking a window of 41 years between 1995 and 2035 (to minimise the effect of global warming on the initial states) we found that the 2015 1st May snapshot (Atmos. A) would rank third in this timeseries.

4. Discussion

There is increasing evidence that the ocean state can be a precursor for the shape of a season to come (Buchan *et al* 2014, Duchez *et al* 2016, Grist *et al* 2019, Hallam *et al* 2019). The recent summers of 2015 and 2018 were both exceptionally hot and dry over much of central Europe (figures 1(b), (c)) and both had a similar temperature anomaly pattern in the northern North Atlantic (figure S6). This raises interesting and important questions about the ocean's potential to contribute to the development of exceptionally warm European summers. Present seasonal forecasting systems—even when they display skill (Scaife *et al* 2014, Dunstone *et al* 2016, Dunstone *et al* 2018)-underestimate extreme seasonal conditions (Baker *et al* 2018). The reasons for this are not yet understood and are topic of ongoing research, but the way forecasting systems are initialised may be a factor. After initialisation by data assimilation, coupled models tend to adjust; they 'repel' the initialised state and drift towards their own attractor. This is particularly troublesome for the subsurface ocean, which is largely adiabatic and data-assimilation introduces artificial sources and sinks. Therefore, the ocean temperature and salinity anomalies that contain a source of predictability may be present in the initial conditions as a consequence of the addition of these artificial sources and sinks of heat (and salt). However, such anomalies may be damped out by adjustment after initialisation shock and the bias/drift correction that is applied in prediction systems that use data-assimilation or full field initialisation. For these reasons we choose to test a gentler initialisation method where neither ocean nor atmospheric initial conditions have been nudged towards observations by artificial sources and sinks. Anomaly fields are taken from an ocean simulation forced by an atmospheric reanalysis, ensuring as much as possible that they are dynamically consistent with the free-running coupled ocean (i.e. structural biases due to the model configuration will be consistent). The conjecture is that this approach reduces model drift and initialisation shocks therefore extending the 'memory' of the ocean in (re-) forecasts.

To keep the number of ensemble simulations within the allocated HPC resources we focused on the impact of the initial states of ocean and atmosphere/sea ice on re-forecasts. It is well known that soil moisture can have a large influence on temperatures over Europe (e.g. Queseda *et al* 2012, Ardilouze *et al* 2017). In our experiments we eliminated the impact of soil moisture by holding it constant. Our results do not conclude that soil moisture did not play a role in the 2015 heatwave. The fact that the summer of 2015 had the lowest precipitation on record (Orth *et al* 2016, figure 1(c)) strongly points to soil moisture aiding the development of the anomalously warm summer of 2015, therefore making soil moisture an ideal candidate for future studies. Furthermore, the sea ice initial conditions used in atmosphere A, B, and C do show a fingerprint of the anthropogenic sea ice decline, with the atmosphere initial condition A having the thinnest sea-ice and bearing closest resemblance to the observed 2015 spring (figure S7). Studies have shown that sea ice can have an impact on temperatures in Europe, especially in winter (e.g. Petoukhov and Semenov 2011) and precipitation in summer (Screen 2013). Preliminary tests indicate that the sea ice initial state is important for the successful re-forecast of summer 2015 (not shown).

Our successful re-forecast of the 2015 heatwave depends on the choice of the initial atmosphere/sea ice condition. The choice of the atmospheric initial conditions is arbitrary and the strong JJA temperature signal signal over central Europe simulated when using the atmosphere state A fortuitous. However, the temperature signal in our re-forecast is clearly statistically significant (30-member ensemble) and larger than the signal obtained in current operational seasonal forecasting systems. Whereas the physical mechanisms that lead to this good result are not yet

fully clear our preliminary assessment is that the initial atmosphere should act to preserve the initial ocean anomalies as well as possible, allowing both for the correct coupled ocean-atmosphere evolution of the initial ocean anomalies and for the correct teleconnections with remote SST anomalies.

To better understand the role of local and remote teleconnections in the successful re-forecast we performed two additional ensembles with 2015 ocean initial condition and atmosphere initial condition A. For these experiments temperature and salinity anomalies are prescribed in the North Atlantic and set to zero elsewhere and vice versa (figure S8). The results suggest a role for both regional (North Atlantic) and remote influence on the development of the warm 2015 JJA anomaly over central Europe (figure S8). In both experiments we find a warm JJA anomaly over central Europe with about half the amplitude of the signal found with atmosphere A and the 2015 ocean. A candidate for remote teleconnections is ENSO.

The prevalent view on the relation between ENSO and European summer climate is that it is weak. However, recently this has been challenged. Rodríguez-Fonseca *et al* (2016) argue that such a relation does exist, but it appears to be non-stationary, modulated by the state of the North Atlantic (AMV) and the characteristics of the ENSO signal (pattern and amplitude). Our results suggest that such a link did exist in spring/summer 2015. Averaged over all ocean initial states, atmosphere initial condition A is still associated with a weaker European heatwave (figure 3). The average over all 4 ocean initial condition SSTs does consist of a positive ENSO signal (figure S1) and atmosphere initial condition A itself consisted of the strongest SAT anomalies over the ENSO-region of all atmospheric initial conditions (figure S2).

We found that a pattern correlation between SST and SAT anomalies in the initial state is a tentative metric for the selection of the atmospheric initial condition. We cannot yet prove that a high pattern correlation to select atmospheric initial conditions systematically improves re-forecasts. Also, it is not yet clear if such an atmospheric state can always be found. Nevertheless, the successful re-forecast using atmosphere initial condition A implies that it is possible to predict the European heatwave of 2015. Preliminary tests using the atmosphere of the UK Met Office's forecasts system did not lead to a better re-forecast than using atmosphere initial condition A (figure S9). Using the initial condition from the forecast still produces a warm anomaly over much of central Europe, however the amplitude of the JJA temperature is only about half of when atmosphere initial condition A is used. This suggests that, when applying the ocean initialisation method studied here, using a model atmosphere analogue may lead to more successful re-forecasts than imposing the observed one which is not part of the model's attractor. Although further testing is needed, our results suggest that our approach outlines a promising route for making seasonal predictions. However, to substantiate these results, further investigation is required before this method can be used in operational prediction systems.

Acknowledgments

N Dunstone, M Andrews, A Duchez, A Scaife, L Jackson, D Copsey, J Grist and S Josey are thanked for all the technical help and/or useful discussion. Model output were post processed on JASMIN, a super-data-cluster to which we are thankful to have access. We acknowledge use of the MONSooN2 system, a collaborative facility supplied under the Joint Weather and Climate Research Programme, a strategic partnership between the UK Met Office and the Natural Environment Research Council. CMAP Precipitation data provided by the NOAA/OAR/ESRL PSD, Boulder, Colorado, USA, from their Web site at https://esrl.noaa.gov/psd/ JVM, JJMH, SSD and ATB were funded by ODYSEA (NE/M006107/1). JVM and SSD also received funding from the EU's Horizon 2020 Research and Innovation Programme under Grant Agreement No 727852 via the project Blue-Action.

Data availability statement

The data that support the findings of this study are openly available at DOI https://doi.org/10.25412/iop.9906620.v1.

ORCID iDs

J V Mecking https://orcid.org/0000-0002-1834-1845

References

Ardilouze C *et al* 2017 Multi-model assessment of the impact of soil moisture initialization on mid-latitude summer predictability *Clim. Dyn.* **49** 3959–74

Baker L H, Shaffrey L C, Sutton R T, Weisheimer A and Scaife A A 2018 An intercomparison of skill and overconfidence/underconfidence of the wintertime North Atlantic Oscillation in multimodel seasonal forecasts *Geophys. Res. Lett.* **45** 7808–17

Ballester J, Rodó X and Giorgi F 2010 Future changes in Central Europe heat waves expected to mostly follow summer mean warming *Clim. Dyn.* **35** 1191–205

Buchan J, Hirschi J J-M, Blaker A T and Sinha B 2014 North Atlantic SST anomalies and the cold North European weather events of winter 2009/10 and December 2010 *Mon. Weather Rev.* **142** 922–32

Ciais P *et al* 2005 Europe-wide reduction in primary productivity caused by the heat and drought in 2003 *Nature* **437** 529–33

Copernicus Climate Change Service (C3S) 2017 ERA5: Fifth generation of ECMWF atmospheric reanalyses of the global climate. Copernicus Climate Change Service Climate Data Store (CDS), 12 August, 2019 (https://cds.climate.copernicus.eu/cdsapp#!/home)

Duchez A, Frajka-Williams E, Josey S A, Evans D G, Grist J P, Marsh R, McCarthy G D, Sinha B, Berry D I and Hirschi J J

2016 Drivers of exceptionally cold North Atlantic Ocean temperatures and their link to the 2015 European heat wave *Environ. Res. Lett.* **11** 074004
Dunstone N *et al* 2018 Skilful seasonal predictions of summer European rainfall *Geophys. Res. Lett.* **45** 3246–54
Dunstone N, Smith D, Scaife A, Hermanson L, Eade R, Robinson N, Andrews M and Knight J 2016 Skilful predictions of the winter North Atlantic Oscillation one year ahead *Nat. Geosci.* **9** 809–14
Feudale L and Shukla J 2011 Influence of sea surface temperature on the European heat wave of 2003 summer: I. An observational study *Clim. Dyn.* **36** 1691–703
Garry F K, McDonagh E L, Blaker A T, Roberts C D, Desbruyères D G, Frajka-Williams E and King B A 2019 Model derived uncertainties in deep ocean temperature trends between 1990-2010 *J. Geophys. Res.* **124** 1155–69
Gastineau G and Frankignoul C 2015 Influence of the North Atlantic SST variability on the atmospheric circulation during the twentieth century *J. Clim.* **28** 1396–416
Grist J P *et al* 2019 Re-emergence of North Atlantic subsurface ocean temperature anomalies in a seasonal forecast system *Clim. Dyn.* 1–22
Grumm R H 2011 The Central European and Russian heat event of July–August 2010 *Bull. Am. Meteorol. Soc.* **92** 1285–96
Hallam S, Marsh R, Josey S A, Hyder P, Moat B and Hirschi J J 2019 Ocean precursors to the extreme Atlantic 2017 hurricane season *Nat. Commun.* **10** 896
Josey S A, Hirschi J J, Sinha B, Duchez A, Grist J P and Marsh R 2018 The recent Atlantic cold anomaly: causes, consequences, and related phenomena *Annu. Rev. Mar. Sci.* **10** 475–501
Kirtman B *et al* 2013 Chapter 11-Near-Term Climate Change: Projections and Predictability *Climate Change 2013: The Physical Science Basis. IPCC Working Group I Contribution to AR5* edited by IPCC (Cambridge: Cambridge University Press)
Lhotka O, Kyselý J and Farda A 2018 Climate change scenarios of heat waves in Central Europe and their uncertainties *Theor. Appl. Clim.* **131** 1043–54
Madec G 2015 NEMO Ocean Engine (https://doi.org/10.5281/zenodo.3248739)
Magnusson L, Balmaseda M A, Corti S, Molteni F and Stockdale T 2013 Evaluation of forecast strategies for seasonal and decadal forecasts in presence of systematic model errors *Clim. Dyn.* **41** 2393–409
Matei D, Pohlmann H, Jungclaus J, Müller W, Haak H and Marotzke J 2012 Two tales of initializing decadal climate prediction experiments with the ECHAM5/MPI-OM model *J. Clim.* **25** 8502–23
Meehl G A and Tebaldi C 2004 More intense, more frequent, and longer lasting heat waves in the 21st century *Science* **305** 994–7
Megann A P, Storkey D, Aksenov Y, Alderson S, Calvert D, Graham T, Hyder P, Siddorn J and Sinha B 2014 GO 5.0: the joint NERC-Met Office NEMO global ocean model for use in coupled and forced applications *Geosci. Model Dev.* **7** 1069–92
Muthers S, Laschewski G and Matzarakis A 2017 The summers 2003 and 2015 in south–west Germany: heat waves and heat-related mortality in the context of climate change *Atmosphere* **8** 224
O'Reilly C H, Heatley J, MacLeod D, Weisheimer A, Palmer T N, Schaller N and Woollings T 2017 Variability in seasonal forecast skill of Northern Hemisphere winters over the 20th Century *Geophys. Res. Lett.* **44** 5729–38
Orth R, Zscheischler J and Seneviratne S I 2016 Record dry summer in 2015 challenges precipitation projections in Central Europe *Sci. Rep.* **6** 28334
Ossó A, Sutton R, Shaffrey L and Dong B 2018 Observational evidence of European summer weather patterns predictable from spring *Proc. Natl Acad. Sci. USA* **115** 59–63
Petoukhov V and Semenov V A 2011 A link between reduced Barents-Kara sea ice and cold winter extremes over Northern Continents *J. Geophys. Res.: Atmos.* **115**
Quesada B, Vautard R, Yiou P and Seneviratne S I 2012 Asymmetric European summer heat predictability from wet and dry southern winters and springs *Nat. Clim. Change* **2** 736–41
Rayner N A, Parker D E, Horton E B, Folland C K, Alexander L V, Rowell D P, Kent E C and Kaplan A 2003 Global analyses of sea surface temperature, sea ice, and night marine air temperature since the late nineteenth century *J. Geophys. Res.* **108** D14
Robine J M, Cheung S L, Le Roy S, Van Oyen H, Griffiths C, Michel J P and Herrmann F R 2008 Death toll exceeded 70 000 in Europe during the Summer of 2003 *C.R. Biol.* **331** 171–8
Rodríguez-Fonseca B, Suárez-Moreno R, Ayarzagüena B, López-Parages J, Gómara I, Villamayor J, Mohino E, Losada T and Castaño-Tierno A 2016 A review of ENSO influence on the North Atlantic. A non-stationary signal *Atmosphere* **7** 87
Russo S, Sillmann J and Fischer E M 2015 Top ten European heatwaves since 1950 and their occurrence in the coming decades *Environ. Res. Lett.* **10** 124003
Scaife A A *et al* 2014 Skillful long-range prediction of European and North American winters *Geophys. Res. Lett.* **41** 2514–9
Schweiger A, Lindsay R, Zhang J, Steele M, Stern H and Kwok R 2011 Uncertainty in modeled Arctic sea ice volume *J. Geophys. Res.* **116** C00D0
Schär C, Vidale P L, Lüthi D, Frei C, Häberli C, Liniger M A and Appenzeller C 2004 The role of increasing temperature variability in European Summer heatwaves *Nature* **427** 332–6
Screen J A 2013 Influence of Arctic sea ice on European summer precipitation *Environ. Res. Lett.* **8**
Sippel S, Otto F E L, Flach M and van Oldenborgh G J 2016 The role of anthropogenic warming in 2015 Central European heat waves *Bull. Am. Meteorol. Soc.* **97** S51–6
Smith D M, Eade R and Pohlmann H 2013 A comparison of full-field and anomaly initialization for seasonal to decadal climate prediction *Clim. Dyn.* **41** 3325–38
Stockdale T N, Molteni F and Ferranti L 2015 Atmospheric initial conditions and the predictability of the Arctic oscillation *Geophys. Res. Lett.* **42** 1173–9
Urban A, Hanzlíková H, Kyselý J and Plavcová E 2017 Impacts of the 2015 heat waves on mortality in the Czech-republic—a comparison with previous heat waves *Int. J. Environ. Res. Publ. Health* **14** E1562
Výberči D, Labudová L, Eštóková M, Faško P and Trizna M 2018 Human mortality impacts of the 2015 Summer heat spells in Slovakia *Theor. Appl. Climatol.* **133** 925–36
Walters D *et al* 2017 The Met Office unified model global atmosphere 6.0/6.1 and JULES global land 6.0/6.1 configurations *Geosci. Model Dev.* **10** 1487–520
Williams K D *et al* 2015 The Met Office global coupled model 2.0 (GC2) configuration *Geosci. Model Dev.* **8** 1509–24
Zampieri M, Ceglar A, Dentener F and Toreti A 2017 Wheat yield loss attributable to heat waves, drought and water excess at the global, national and subnational scales *Environ. Res. Lett.* **12** 64008